ACS APPLIED MATERIALS & INTERFACES

Research Article

www.acsami.org

Colorimetric Peroxidase Mimetic Assay for Uranyl Detection in Sea Water

Dingyuan Zhang, Zhuo Chen, Haneen Omar, Lin Deng, and Niveen M. Khashab*

Controlled Release and Delivery Lab, Advanced Membranes and Porous Materials Center, King Abdullah University of Science and Technology, Thuwal 23955-6900, Kingdom of Saudi Arabia

Supporting Information

ABSTRACT: Uranyl (UO_2^{2+}) is a form of uranium in aqueous solution that represents the greatest risk to human health because of its bioavailability. Different sensing techniques have been used with very sensitive detection limits especially the recently reported uranyl-specific DNAzymes systems. However, to the best of our knowledge, few efficient detection methods have been reported for uranyl sensing in seawater. Herein, gold nanoclusters (AuNCs) are employed in an efficient spectroscopic method to detect uranyl ion (UO_2^{2+}) with a detection limit of 1.86 μM. In the absence of UO_2^{2+}, the BSA-stabilized AuNCs (BSA-AuNCs) showed an intrinsic peroxidase-like activity. In the presence of UO_2^{2+}, this activity can be efficiently restrained. The preliminary quenching mechanism and selectivity of UO_2^{2+} was also investigated and compared with other ions. This design strategy could be useful in understanding the binding affinity of protein-stabilized AuNCs to UO_2^{2+} and consequently prompt the recycling of UO_2^{2+} from seawater.

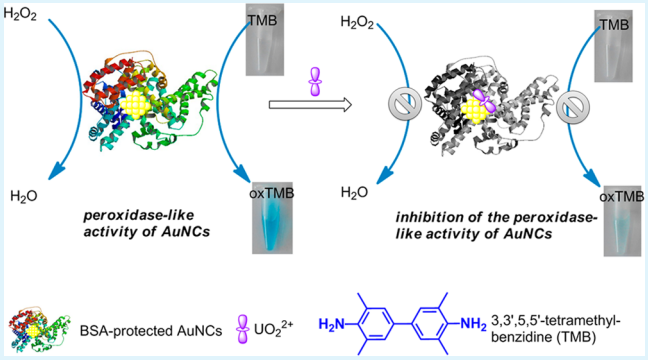

KEYWORDS: *gold nanoclusters, uranyl, peroxidase mimetic, sensors, seawater, proteins*

INTRODUCTION

Uranium represents an important source of nuclear-energy fuel. Since the direct disposal of spent fuel in a nuclear waste repository can contaminate the groundwater and seawater, the assessment of water contamination is a crucial environmental concern. Uranyl (UO_2^{2+}) represents the most stable uranium ion in aerobic environments and is considered as a highly toxic carcinogen.[1−3] Desalination of seawater is the major source of portable and drinking water in many countries including saudi arabia. Therefore, it is of high importance to detect the uranyl level in biological fluids and natural water. So far, extensive detection methods for uranyl have been reported including atomic absorption spectrometry,[4] phosphorescence,[5] inductively coupled plasma mass spectrometry,[6,7] and Raman spectroscopy.[8] Colorimetric detection using nanoparticles offers a straightforward method to detect contaminants by the naked eye.[9−14] Recent reports have utilized uranyl-specific DNAzymes on the surface of gold nanoparticles as efficient uranyl sensors.[15−18] Although these systems have impressive detection levels, they are limited by the complicated DNAzyme fabrication. Thus, it is still of continued interest and great importance to explore simple and efficient detecting approaches for uranium, especially in seawater where many uranyl ion complexes can be present.

Recently, the intrinsic enzyme-like activity of nanomaterials has become a growing area of interest in specific and sensitive biomolecular and heavy metal detection. Several kinds of nanomaterials, such as Fe_3O_4 nanoparticles,[19,20] graphene oxide,[21] carbon nanotubes,[22] gold nanoparticles,[23] silver nanoparticles,[24] carbon nanodots,[25] graphitic carbon nitride nanosheets,[26] and TiO_2 nanotube arrays,[27] etc., have been established as highly stable and low-cost alternatives to natural enzymes, which could directly catalyze the oxidation of the corresponding substrates to achieve visual detections.

Metal nanoclusters (NCs), with a core size below 2 nm, have been recently investigated for their highly intrinsic peroxidase-like activity. Possessing molecule-like properties, protein templated gold nanoclusters have shown promise for diverse applications such as sensing, bioimaging, and also in cancer therapy.[28−36] Compared to previous reports on nanomaterial-based peroxidase mimetics, the efficient utilization of bovine serum albumin-stabilized gold NCs (BSA-AuNCs) in bioanalysis relies on their ultrasmall size, excellent stability, and biocompatibility in aqueous solution.[37−39] Inspired by these reports and in continuation with our research interest in the application of AuNCs, we investigated the intrinsic peroxidase-like activity of AuNCs toward uranyl. Herein, we developed a simple, reliable, and selective colorimetric sensing technique of uranyl by utilizing BSA-AuNCs as a novel platform.

Received: October 31, 2014
Accepted: February 6, 2015
Published: February 6, 2015

DOI: 10.1021/am507361x
ACS Appl. Mater. Interfaces 2015, 7, 4589−4594

Scheme 1. Sensing Principle of Uranyl Ion Sensor via Inhibiting BSA-AuNCs Peroxidase Activity

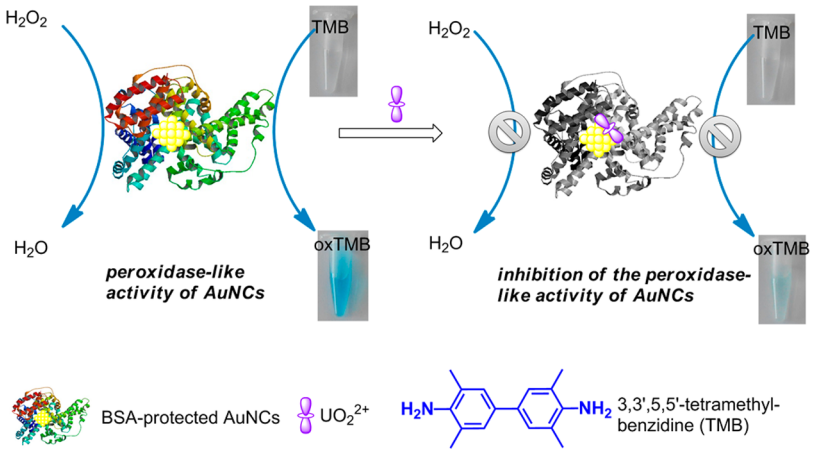

The designed system is illustarted in Scheme 1. BSA-AuNCs show strong peroxidase activity, which is most probably considered to come from transitions of free electrons of AuNCs.[40] The detection mechanism is based on that TMB (3,3′,5,5′-tetramethylbenzidine) is quickly converted into a blue charge-transfer complex (chromogen) in the presence of BSA-AuNCs and H_2O_2[41] while the presence of UO_2^{2+} effectively inhibits the peroxidase-like activity of BSA-AuNCs (Scheme 1). To the best of our knowledge, our method is the first example employing the interaction between UO_2^{2+} and AuNCs to set up a facile colorimetric uranyl sensor with good sensitivity and excellent selectivity.

EXPERIMENTAL SECTION

Caution! *^{238}U, which is a low specific-activity α-particle emitting radionuclide, presents potential harm to human health.[1−3] This toxic and radioactive material should be used with extreme care.*

Reagents and Materials. Milli-Q water (18.2 mΩ·cm, 25°C; Millpore Co., USA) was used in all experiments and to prepare all buffers. Sodium hydroxide (NaOH), bovine serum albumin (BSA), 3,3′,5,5′-tetramethylbenzidine (TMB), hydrogen peroxide solution (H_2O_2, 30 wt % aqueous), and chloroauric acid ($HAuCl_4{\cdot}4H_2O$) were purchased from Sigma-Aldrich. All the chemicals were used as received without further purification. Sea water was obtained from the Red Sea near King Abdullah University of Science and Technology.

Characterizations. Fluorescence measurements were carried out on a Cary Eclipse fluorescence spectrophotometer (Varian). The excitation and emission slits were set at 10 nm. Absorbance spectra were acquired on a Cary-5000 UV−vis-NIR spectrophotometer (Varian) by using a 1 cm path length cell. Transmission electron microscopic (TEM) experiments were performed using a FEI Tacnai 12 microscope operating at 120 kV. For visualization by TEM, samples were prepared by dropping the solution onto a carbon-coated copper grid. FTIR spectra were recorded on a Thermo Nicolet 6700 FT-IR system. Circular dichroism (CD) spectra were acquired by using a Jasco J-820 spectropolarimeter with a computer-controlled water bath.[4]

Synthesis of BSA-AuNCs. BSA-AuNCs were prepared following previous method.[42] All glassware were washed with Aqua Regia (HCl/HNO_3 = 3/1, v/v), then rinsed with Milli-Q water. Typically, 5 mL aqueous $HAuCl_4$ solution (10 mM, 37 °C) was added to BSA solution (5 mL, 50 mg/mL, 37 °C) under vigorous stirring. NaOH solution (0.5 mL, 1 M) was later added and the mixture was incubated at 37 °C for 12 h. The final BSA-AuNCs solution was kept at 4 °C prior to use.

Uranyl Sensing Based on Inhibiting BSA-AuNCs Peroxidase Activity. In a typical test, BSA-AuNCs solution (25 μL, pH 7) in 275 μL buffer solution (25 mM Na_2HPO_4, pH 5.0) was first mixed with different concentrations of UO_2^{2+} (100 μL) at 37 °C. The mixture was incubated at 37 °C for 10 min. A sequence of solutions, 50 μL of TMB (final concentration 0.5 mM) and 50 μL of H_2O_2 (final concentration 10 mM), were then added to 300 μL of as prepared AuNCs/UO_2^{2+} mixture. After 30 min incubation, the inhibition of peroxidase activity was measured by monitoring the absorbance change at 652 nm with a Cary-5000 UV−vis−NIR spectrophotometer (Varian) spectrophotometer.

RESULTS AND DISCUSSION

Protein templated AuNCs are synthesized using bovine serum albumin (BSA) as reported.[42] The average diameter of as-synthesized AuNCs is about 2.33 nm, as shown by transmission electron microscopy (TEM) (Figure S1 and S2, Supporting Information). Fluorescence and FT-IR spectra are in agreement with literature reports and are presented in Supporting Information Figures S3 and S4, respectively.[42]

To evaluate the peroxidase-like activity TMB, a peroxidase susbstrate, was used. In the presence of H_2O_2, TMB can be easily oxidized producing a blue color with maximum absorbance at 652 nm.[43] Figure 1 shows the absorption spectra of three different reaction systems after 30 min. BSA-AuNCs can catalyze the oxidation of TMB in the presence of H_2O_2 to generate a bright blue color (curve a, Figure 1). With the injection of UO_2^{2+}, the catalytic activity of AuNCs quickly decreased because of the inhibiting function of UO_2^{2+} (curve b, Figure 1). However, negligible color variation was observed for TMB-H_2O_2 solution in the absence of BSA-AuNCs (curve c, Figure 1).

The optimization of the sensing conditions, including pH, temperature, time, BSA-AuNCs, TMB, and H_2O_2 concentration, was then investigated. To optimize the detecting conditions, A_0/A was used as a criterion, where A0 and A represent the absorbance in the absence and presence of UO_2^{2+}, respectively. After a series of experiments, including variation of reaction temperature, pH, time, and the ratio of BSA-AuNCs/TMB/H_2O_2, the optimal sensing conditions were obtained when the reaction of H_2O_2 (10.0 mM) and TMB (0.5 mM) was performed with BSA-AuNCs (200 μM) in the presence of UO_2^{2+} in pH 5.0 buffer at 37 °C for the incubation time of 30 min (Supporting Information Figure S5−10).

To evaluate the sensitivity of this UO_2^{2+} detecting system, the changes of absorbance were monitored with injection of different concentrations of UO_2^{2+} under the optimized experimental conditions. As illustrated in Figure 2A, the absorbance at 652 nm (A652) decreased gradually when the

DOI: 10.1021/am507361x
ACS Appl. Mater. Interfaces 2015, 7, 4589−4594

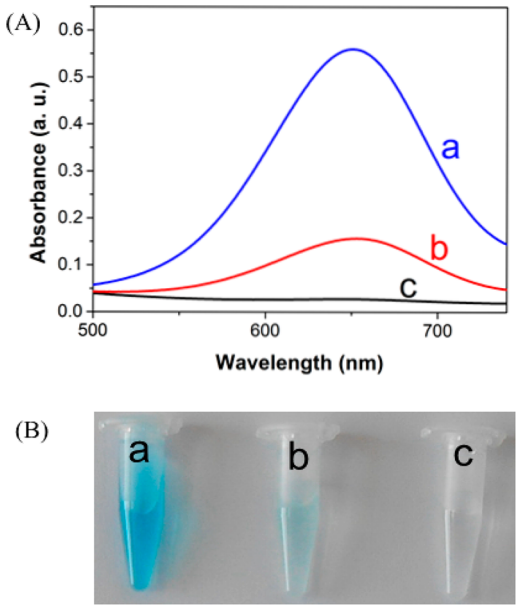

Figure 1. (A) Absorption spectra and (B) photographs of inhibiting effects of UO_2^{2+} on the peroxidase mimetic activity of BSA-AuNCs: (a) 0.5 mM TMB + 10 mM H_2O_2 + 200 μM BSA-AuNCs; (b) 0.5 mM TMB + 10 mM H_2O_2 + 200 μM BSA-AuNCs + 50 μM UO_2^{2+}; (c) 0.5 mM TMB + 10 mM H_2O_2; pH = 5.0.

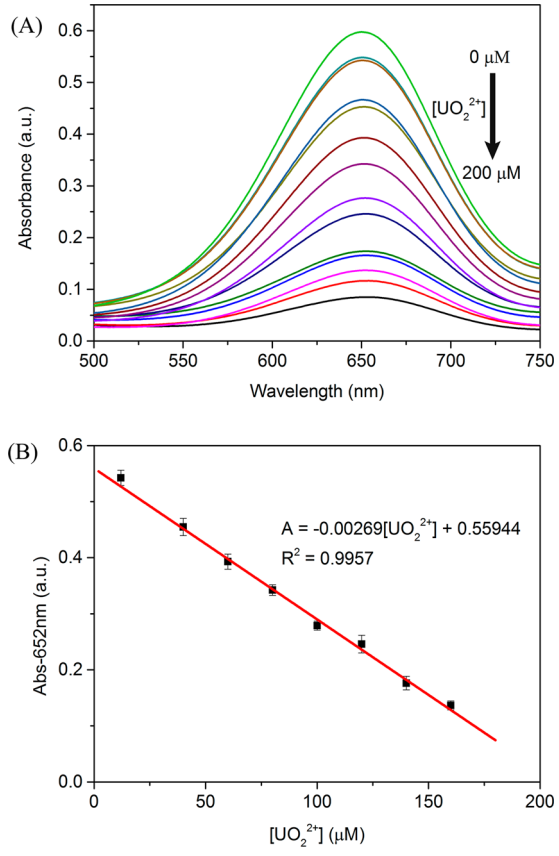

Figure 2. (A) UV−vis absorption spectra, UO_2^{2+}concentrations were 0−200 μM; (B) linear calibration plot for UO_2^{2+}detection.; UO_2^{2+} concentrations were 12−160 μM; BSA-AuNCs, 200 μM; TMB, 0.5 mM; H_2O_2, 10 mM; temperature, 37 °C; pH 5.0. (n = 5).

concentration of UO_2^{2+} was raised from 0 to 200 μM, suggesting that the changes of absorbance could be employed for the quantitative sensing of UO_2^{2+}. It is shown that a good linear relationship between A652 and UO_2^{2+} concentration over the range of 12−160 μM can be acquired as demonstrated in Figure 2B (A652 was plotted as a function of UO_2^{2+} concentration). The linear equation is $A = -0.00269[UO_2^{2+}] + 0.55944$, where $[UO_2^{2+}]$ is the UO_2^{2+} concentration and A is the absorbance intensity at 652 nm, $R^2 = 0.9957$. The detection limit of UO_2^{2+} is then determined to be 1.86 μM with a signal-to-noise ratio of 3.

To further investigate the selectivity of this detection system, other ions were tested including Na^+, Fe^{3+}, Co^{2+}, Li^+, Al^{3+}, K^+, Ca^{2+}, Cu^{2+}, Zn^{2+}, Pb^{2+}, I^-, and S^{2-} (cyan column, Figure 3) at a concentration of 50 μM under the same conditions. UO_2^{2+} resulted in a significant inhibitation in the peroxidase-like activity of BSA-AuNCs (pink column, Figure 3). No apparent effect was observed with most metal ions except for Hg^{2+} and Ag^+, predictably.[37] Potassium iodide (20 μM) was then used to form a stable masking reagent and successfully masked the response of the assay to Hg^{2+} and Ag^+(gray column, Figure 3). These results clearly confirm that the BSA-AuNCs-based UO_2^{2+} sensor is highly selective.

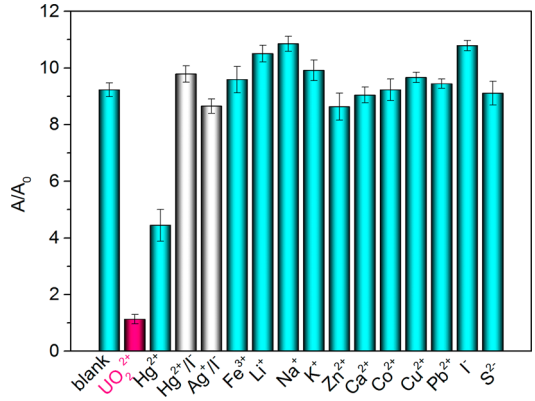

Figure 3. Effect of ions on inhibiting the peroxidase-like activity of BSA-AuNCs. **A** presents absorbance intensity at 652 nm of different ion samples, $\mathbf{A_0}$ presents absorbance intensity at 652 nm of the UO_2^{2+} sample. Concentration of UO_2^{2+} (pink column), Hg^{2+}, Fe^{3+}, Li^+, Na^+, K^+, Zn^{2+}, Ca^{2+}, Co^{2+}, Cu^{2+}, Pb^{2+}, I^-, S^{2-} (cyan column) are 50 μM; Hg^{2+} and Ag^+ in the presence of 20 μM KI as the masking reagent (gray column); BSA-AuNCs, 200 μM; TMB, 0.5 mM; H_2O_2, 10 mM; temperature, 37 °C; pH 5.0 (n = 5).

Uranyl selective inhibition of BSA-AuNCs peroxidase-like activity suggests that our detecting approach might be applied for measuring uranyl concentration in seawater samples. As a proof of concept, seawater samples were injected with $UO_2(OAc)_2$. The samples were analyzed by UV−vis spectroscopy by applying a calibration plot. All water samples from red sea were diluted 10 times with PBS (pH 7.4) before testing because of their extremly high salt concentration. Moreover, different concentrations of UO_2^{2+} solution were injected into the corresponding TMB-H_2O_2 and BSA-AuNCs solutions to test the recovery and standard deviation (R.S.D.) as shown in Table 1. This proves that our approach can be efficiently employed for the determination of UO_2^{2+} in seawater samples.

FT-IR reveals that the existence of UO_2^{2+} can change the structure of BSA-AuNCs, in which a new peak at 1100 cm^{-1} appeared for carbon−oxygen single bond, which suggests that UO_2^{2+} may interact with some primary or secondary hydroxyl groups in BSA (Figure 4A).[48,49] This feature was further

DOI: 10.1021/am507361x
ACS Appl. Mater. Interfaces 2015, 7, 4589−4594

Table 1. Quantitative Determination of UO_2^{2+} in $UO_2(OAc)_2$ Injected in Red Sea Samples[a]

no.	added (μM)	measured (μM)	recovery (%)	RSD (%, n = 5)
1	10.0	9.8	98	3.0
2	20.0	20.8	104	5.1
3	40.0	41.4	103	4.5
4	80.0	78.4	98	5.7

[a]Red Sea samples were diluted 10 times with PBS (pH 7.4) before measurement. Concentration of UO_2^{2+} injection in seawater sample; BSA-AuNCs, 200 μM; TMB, 0.5 mM; H_2O_2, 10 mM; temperature, 37 °C; pH 5.0 (n = 5).

confirmed by the UV−vis absorbance spectra of BSA-AuNCs (black dashed line) and BSA-AuNCs with UO_2^{2+} (red solid line), BSA-AuNCs has a a small absorbance peak at 280 nm, while in the prensece of UO_2^{2+}, a wide peak from 200 to 395 nm and a small peak at 430 nm were observed (Figure 4B). In addition, the binding affinity of the BSA-AuNCs toward UO_2^{2+} was measured by Circular Dichroism (CD) (Figure 4C), in which it shows a red-shift of up to 2 nm of the characteristic BSA-AuNCs peak (190 nm). The fabrication of the sensing platform was further validated by UV kinetic curves, where UO_2^{2+} can decrease the intrinsic peroxidase-like activity of the BSA-AuNCs (Figure 4D). The presence of UO_2^{2+} leads to the fusion of AuNCs which eventually aggregate as verified by the TEM results (Supporting Information Figure S1b). We also investigated the fluorescence spectrum of BSA-AuNCs in the presence of different concentration of UO_2^{2+} from 0 to 5 mM. With the increasing concentration of UO_2^{2+}, the photoemission peak at 645 nm decreased gradually, which also confirmed that UO_2^{2+} can interact with BSA-AuNCs (Supporting Information Figure S11). On the basis of these results, we verified that the mechanism for the sensitive peroxidase-like activity response is due to a dynamic uranyl−BSA interaction process rather than a simple electrostatic interaction between these moieties.

Research on UO_2^{2+} binding to protein has created a new way to recognize and recycle UO_2^{2+} based on biocoordination chemistry.[44−47] UO_2^{2+} has a unique structure of a linear dioxocation with a formal charge of +2, where the use of common chelating ligands that bind to spherical cations in three dimensions shows ineffective, such as EDTA and DTPA.[48] Very recently, a stable protein targeting uranyl with high selectivity was developed via a computational screening strategy.[49] We hypothesize that the mechanism of UO_2^{2+} interacting with BSA-AuNCs could be similar to that of the uranyl specific designed protein in terms of its ability to biocoordinate. On the other hand, various novel materials such as metal−organic frameworks (MOFs), silver nanoparticles embedded polymer, have been applied for removing and recovering of uranyl.[50−53] Our results indicate that BSA-AuNCs could also be used as a functional platform for simultaneous sensing and extraction of uranyl.

CONCLUSION

In summary, a versatile and selective colorimetric detection method for uranyl has been successfully demonstrated. The detection mechanism is based on that uranyl could inhibit the strong intrinsic peroxidase-like activity of BSA-AuNCs. The disappearence of the blue color can readily act as a visual detection method. Moreover, the proposed approach is

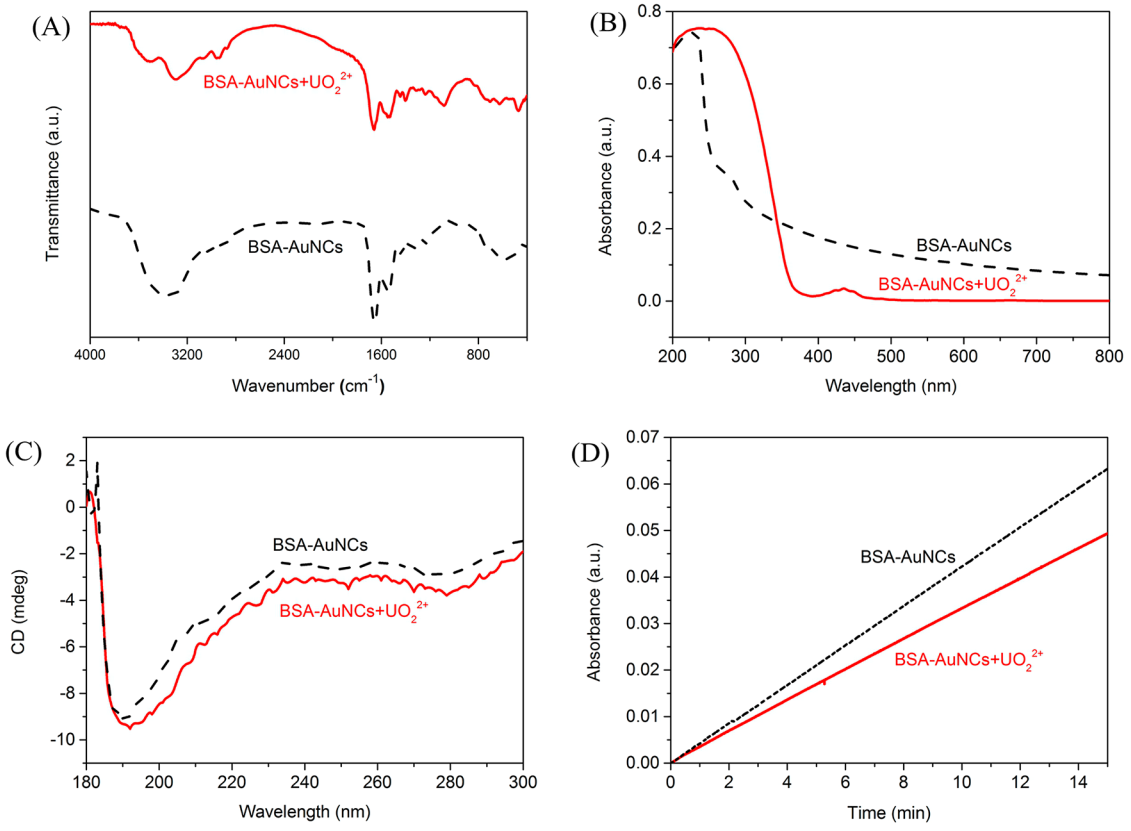

Figure 4. (A) FTIR spectra, (B) UV−vis absorbance, (C) circular dichroism, and (D) UV−vis kinetic curve of BSA-AuNCs (black dashed line) and BSA-AuNCs with UO_2^{2+} (red solid line).

DOI: 10.1021/am507361x
ACS Appl. Mater. Interfaces 2015, 7, 4589−4594

efficiently used for the quantitative determination of uranyl in seawater. The colorimetric strategy based on BSA-AuNCs has the potential to act as a new uranyl sensing system with low cost and high selectivity. More elaborate designs are currently underway to improve the sensitivity of this technique, while maintaining the simplicity and efficiency of preparation and application.

■ ASSOCIATED CONTENT

Supporting Information

Additional information about characterization, figures showing TEM of Au-NCs, size distribution histogram of BSA-AuNCs, photoemission and photoexcitation spectra of aqueous solution of BSA-AuNCs, FTIR of BSA-AuNCs and BSA, Optimization of pH, TMB concentration, H_2O_2 concentration, BSA-AuNCs concentration, reaction time, and temperature for UO_2^{2+} detection, photoemission spectrum of BSAAuNCs in the presence of UO_2^{2+}, a table showing a comparison of different fluorescent methods for UO_2^{2+} detection, and additional references. This material is available free of charge via the Internet at http://pubs.acs.org.

■ AUTHOR INFORMATION

Corresponding Author

*Tel: +966-28021172. Fax: +966-28082410. E-mail: Niveen.khashab@kaust.edu.sa.

Author Contributions

The manuscript was written through contributions of all authors. All authors have given approval to the final version of the manuscript.

Notes

The authors declare no competing financial interest.

■ ACKNOWLEDGMENTS

The authors gratefully acknowledge King Abdullah University of Science and Technology (KAUST) for the support of this work.

■ REFERENCES

(1) Briner, W. The Toxicity of Depleted Uranium. *Int. J. Environ. Res. Publ. Health* **2010**, *7*, 303−313.
(2) Craft, E. S.; Abu-Qare, A. W.; Flaherty, M. M.; Garofolo, M. C.; Rincavage, H. L.; Abou-Donia, M. B. Depleted and Natural Uranium: Chemistry and Toxicological Effects. *J. Toxicol. Environ. Health, Part B* **2004**, *7*, 297−317.
(3) Domingo, J. L. Reproductive and Developmental Toxicity of Natural and Depleted Uranium: a Review. *Reprod. Toxicol.* **2001**, *15*, 603−609.
(4) Abbasi, S. A. Atomic Absorption Spectrometric and Spectrophotometric Trace Analysis of Uranium in Environmental Samples with *N*-*p*-Methoxyphenyl-2-Furylacrylohydroxamic acid and 4-(2-Pyridylazo) Resorcinol. *Int. J. Environ. Anal. Chem.* **1989**, *36*, 163−172.
(5) Brina, R.; Miller, A. G. Direct Detection of Trace Levels of Uranium by Laser-Induced Kinetic Phosphorimetry. *Anal. Chem.* **1992**, *64*, 1413−1418.
(6) Lorber, A.; Karpas, Z.; Halicz, L. Flow Injection Method for Determination of Uranium in Urine and Serum by Inductively Coupled Plasma Mass Spectrometry. *Anal. Chim. Acta* **1996**, *334*, 295−301.
(7) Rani, A.; Mehra, R.; Duggal, V.; Balaram, V. Analysis of Uranium Concentration in Drinking Water Samples Using ICPMS. *Health Phys.* **2013**, *104*, 251−255.
(8) Ruan, C.; Luo, W.; Wang, W.; Gu, B. Surface-Enhanced Raman Spectroscopy for Uranium Detection and Analysis in Environmental Samples. *Anal. Chim. Acta* **2007**, *605*, 80−86.
(9) Du, J.; Jiang, L.; Shao, Q.; Liu, X.; Marks, R. S.; Ma, J.; Chen, X. Colorimetric Detection of Mercury Ions Based on Plasmonic Nanoparticles. *Small* **2013**, *9*, 1467−1481.
(10) Du, J.; Zhu, B.; Peng, X.; Chen, X. Optical Reading of Contaminants in Aqueous Media Based on Gold Nanoparticles. *Small* **2014**, *10*, 3461−3479.
(11) Lee, J.-S.; Han, M. S.; Mirkin, C. A. Colorimetric Detection of Mercuric Ion(Hg^{2+}) in Aqueous Media Using DNA-Functionalized Gold Nanoparticles. *Angew. Chem., Int. Ed.* **2007**, *46*, 4093−4096.
(12) Du, J.; Sun, Y.; Jiang, L.; Cao, X.; Qi, D.; Yin, S.; Ma, J.; Boey, F. Y. C.; Chen, X. Flexible Colorimetric Detection of Mercuric Ion by Simply Mixing Nanoparticles and Oligopeptides. *Small* **2011**, *7*, 1407−1411.
(13) Du, J.; Shao, Q.; Yin, S.; Jiang, L.; Ma, J.; Chen, X. Colorimetric Chemodosimeter Based on Diazonium-Gold-Nanoparticle Complexes for Sulfite Ion Detection in Solution. *Small* **2012**, *8*, 3412−3416.
(14) Du, J.; Zhu, B.; Chen, X. Urine for Plasmonic Nanoparticle-Based Colorimetric Detection of Mercury Ion. *Small* **2013**, *9*, 4104−4111.
(15) Liu, J.; Brown, A. K.; Meng, X.; Cropek, D. M.; Istok, J. D.; Watson, D. B.; Lu, Y. A Catalytic Beacon Sensor for Uranium with Parts-per-Trillion Sensitivity and Million-fold Selectivity. *Natl. Acad. Sci. U. S. A.* **2007**, *104*, 2056−2061.
(16) Lee, J. H.; Wang, Z.; Liu, J.; Lu, Y. Highly Sensitive and Selective Colorimetric Sensors for Uranyl(UO_2^{2+}): Development and Comparison of Labeled and Label-Free DNAzyme-Gold Nanoparticle Systems. *J. Am. Chem. Soc.* **2008**, *130*, 14217−14226.
(17) Liu, J.; Lu, Y. Rational Design of "Turn-On" Allosteric DNAzyme Catalytic Beacons for Aqueous Mercury Ions with Ultrahigh Sensitivity and Selectivity. *Angew. Chem., Int. Ed.* **2007**, *46*, 7587−7590.
(18) Wu, P.; Hwang, K.; Lan, T.; Lu, Y. A DNAzyme-Gold Nanoparticle Probe for Uranyl Ion in Living Cells. *J. Am. Chem. Soc.* **2013**, *135*, 5254−5257.
(19) Wei, H.; Wang, E. Fe_3O_4 Magnetic Nanoparticles as Peroxidase Mimetics and Their Applications in H_2O_2 and Glucose Detection. *Anal. Chem.* **2008**, *80*, 2250−2254.
(20) Gao, L.; Zhuang, J.; Nie, L.; Zhang, J.; Zhang, Y.; Gu, N.; Wang, T.; Feng, J.; Yang, D.; Perrett, S.; Yan, X. Intrinsic Peroxidase-Like Activity of Ferromagnetic Nanoparticles. *Nat. Nanotechnol.* **2007**, *2*, 577−583.
(21) Song, Y.; Qu, K.; Zhao, C.; Ren, J.; Qu, X. Graphene Oxide: Intrinsic Peroxidase Catalytic Activity and Its Application to Glucose Detection. *Adv. Mater.* **2010**, *22*, 2206−2210.
(22) Song, Y.; Wang, X.; Zhao, C.; Qu, K.; Ren, J.; Qu, X. Label-Free Colorimetric Detection of Single Nucleotide Polymorphism by Using Single-Walled Carbon Nanotube Intrinsic Peroxidase-Like Activity. *Chem.—Eur. J.* **2010**, *16*, 3617−3621.
(23) Jv, Y.; Li, B.; Cao, R. Positively-Charged Gold Nanoparticles as Peroxidase Mimic and Their Application in Hydrogen Peroxide and Glucose Detection. *Chem. Commun.* **2010**, *46*, 8017−8019.
(24) Jiang, H.; Chen, Z.; Cao, H.; Huang, Y. Peroxidase-like activity of Chitosan Stabilized Silver Nanoparticles for Visual and Colorimetric Detection of Glucose. *Analyst* **2012**, *137*, 5560−5564.
(25) Shi, W.; Wang, Q.; Long, Y.; Cheng, Z.; Chen, S.; Zheng, H.; Huang, Y. Carbon Nanodots as Peroxidase Mimetics and Their Applications to Glucose Detection. *Chem. Commun.* **2011**, *47*, 6695−6697.
(26) Tian, J.; Liu, Q.; Asiri, A. M.; Qusti, A. H.; Al-Youbi, A. O.; Sun, X. Ultrathin Graphitic Carbon Nitride Nanosheets: a Novel Peroxidase Mimetic, Fe Doping-Mediated Catalytic Performance Enhancement and Application to Rapid, Highly Sensitive Optical Detection of Glucose. *Nanoscale* **2013**, *5*, 11604−11609.
(27) Zhang, L.; Han, L.; Hu, P.; Wang, L.; Dong, S. TiO_2 Nanotube Arrays: Intrinsic Peroxidase Mimetics. *Chem. Commun.* **2013**, *49*, 10480−10482.

DOI: 10.1021/am507361x
ACS Appl. Mater. Interfaces 2015, 7, 4589−4594

(28) Liu, G.; Shao, Y.; Wu, F.; Xu, S.; Peng, J.; Liu, L. DNA-Hosted Fluorescent Gold Nanoclusters: Sequence-Dependent Formation. *Nanotechnology* **2013**, *24*, No. 015503.
(29) Huang, C.-C.; Yang, Z.; Lee, K.-H.; Chang, H.-T. Synthesis of Highly Fluorescent Gold Nanoparticles for Sensing Mercury(II). *Angew. Chem., Int. Ed.* **2007**, *46*, 6824−6828.
(30) Jin, L.; Shang, L.; Guo, S.; Fang, Y.; Wen, D.; Wang, L.; Yin, J.; Dong, S. Biomolecule-Stabilized Au Nanoclusters as a Fluorescence Probe for Sensitive Detection of Glucose. *Biosens. Bioelectron.* **2011**, *26*, 1965−1969.
(31) Lin, Y.-H.; Tseng, W.-L. Ultrasensitive Sensing of Hg^{2+} and CH_3Hg^+ Based on the Fluorescence Quenching of Lysozyme Type VI-Stabilized Gold Nanoclusters. *Anal. Chem.* **2010**, *82*, 9194−9200.
(32) Liu, Y.; Ai, K.; Cheng, X.; Huo, L.; Lu, L. Gold-Nanocluster-Based Fluorescent Sensors for Highly Sensitive and Selective Detection of Cyanide in Water. *Adv. Funct. Mater.* **2010**, *20*, 951−956.
(33) Wei, H.; Wang, Z.; Yang, L.; Tian, S.; Hou, C.; Lu, Y. Lysozyme-Stabilized Gold Fluorescent Cluster: Synthesis and Application as Hg^{2+} Sensor. *Analyst* **2010**, *135*, 1406−1410.
(34) Xie, J.; Zheng, Y.; Ying, J. Y. Highly Selective and Ultrasensitive Detection of Hg^{2+} Based on Fluorescence Quenching of Au Nanoclusters by Hg^{2+}−Au^+ Interactions. *Chem. Commun.* **2010**, *46*, 961−963.
(35) Hu, L.; Deng, L.; Alsaiari, S.; Zhang, D.; Khashab, N. M. "Light-on" Sensing of Antioxidants Using Gold Nanoclusters. *Anal. Chem.* **2014**, *86*, 4989−4994.
(36) Hu, L.; Han, S.; Parveen, S.; Yuan, Y.; Zhang, L.; Xu, G. Highly Sensitive Fluorescent Detection of Trypsin-Based on BSA-Stabilized Gold Nanoclusters. *Biosens. Bioelectron.* **2012**, *32*, 297−299.
(37) Zhu, R.; Zhou, Y.; Wang, X.-L.; Liang, L.-P.; Long, Y.-J.; Wang, Q.-L.; Zhang, H.-J.; Huang, X.-X.; Zheng, H.-Z. Detection of Hg^{2+} Based on the Selective Inhibition of Peroxidase Mimetic Activity of BSA−Au Clusters. *Talanta* **2013**, *117*, 127−132.
(38) Liu, P.; Shang, L.; Li, H.; Cui, Y.; Qin, Y.; Wu, Y.; Hiltunen, J. K.; Chen, Z.; Shen, J. Synthesis of Fluorescent α-Chymotrypsin A-Functionalized Gold Nanoclusters and Their Application to Blot-Based Technology for Hg^{2+} Detection. *RSC Adv.* **2014**, *4*, 31536−31543.
(39) Zhao, Q.; Chen, S.; Huang, H.; Zhang, L.; Wang, L.; Liu, F.; Chen, J.; Zeng, Y.; Chu, P. K. Colorimetric and Ultra-Sensitive Fluorescence Resonance Energy Transfer Determination of H_2O_2 and Glucose by Multi-Functional Au Nanoclusters. *Analyst* **2014**, *139*, 1498−1503.
(40) Zheng, J.; Nicovich, P. R.; Dickson, R. M. Highly Fluorescent Noble Metal Quantum Dots. *Annu. Rev. Phys. Chem.* **2007**, *58*, 409−431.
(41) Guo, Y.; Deng, L.; Li, J.; Guo, S.; Wang, E.; Dong, S. Hemin-Graphene Hybrid Nanosheets with Intrinsic Peroxidase-like Activity for Label-free Colorimetric Detection of Single-Nucleotide Polymorphism. *ACS Nano* **2011**, *5*, 1282−1290.
(42) Xie, J.; Zheng, Y.; Ying, J. Y. Protein-Directed Synthesis of Highly Fluorescent Gold Nanoclusters. *J. Am. Chem. Soc.* **2009**, *131*, 888−889.
(43) Marquez, L. A.; Dunford, H. B. Mechanism of the Oxidation of 3,5,3′,5′-Tetramethylbenzidine by Myeloperoxidase Determined by Transient- and Steady-State Kinetics. *Biochemistry* **1997**, *36*, 9349−9355.
(44) Wegner, S. V.; Boyaci, H.; Chen, H.; Jensen, M. P.; He, C. Engineering a Uranyl-Specific Binding Protein from NikR. *Angew. Chem., Int. Ed.* **2009**, *48*, 2339−2341.
(45) Vidaud, C.; Gourion-Arsiquaud, S.; Rollin-Genetet, F.; Torne-Celer, C.; Plantevin, S.; Pible, O.; Berthomieu, C.; Quemeneur, E. Structural Consequences of Binding of UO_2^{2+} to Apotransferrin: Can This Protein Account for Entry of Uranium into Human Cells? *Biochemistry* **2007**, *46*, 2215−2226.
(46) Pible, O.; Guilbaud, P.; Pellequer, J. L.; Vidaud, C.; Quemeneur, E. Structural Insights into Protein−Uranyl Interaction: Towards an in Silico Detection Method. *Biochimie* **2006**, *88*, 1631−1638.
(47) Qi, L.; Basset, C.; Averseng, O.; Quemeneur, E.; Hagege, A.; Vidaud, C. Characterization of UO_2^{2+} Binding to Osteopontin, A Highly Phosphorylated Protein: Insights into Potential Mechanisms of Uranyl Accumulation in Bones. *Metallomics* **2014**, *6*, 166−176.
(48) Cantat, T.; Arliguie, T.; Noel, A.; Thuery, P.; Ephritikhine, M.; Le Floch, P.; Mezailles, N. The U═C Double Bond: Synthesis and Study of Uranium Nucleophilic Carbene Complexes. *J. Am. Chem. Soc.* **2009**, *131*, 963−972.
(49) Zhou, L.; Bosscher, M.; Zhang, C.; Ozcubukcu, S.; Zhang, L.; Zhang, W.; Li, C. J.; Liu, J.; Jensen, M. P.; Lai, L.; He, C. A Protein Engineered to Bind Uranyl Selectively and With Femtomolar Affinity. *Nat. Chem.* **2014**, *6*, 236−241.
(50) Sayin, S.; Yilmaz, M. Preparation and Uranyl Ion Extraction Studies of Calix 4 Arene-Based Magnetite Nanoparticles. *Desalination* **2011**, *276*, 328−335.
(51) Ulusoy, H. I.; Simsek, S. Removal of Uranyl Ions in Aquatic Mediums by Using a New Material: Gallocyanine Grafted Hydrogel. *J. Hazard. Mater.* **2013**, *254*, 397−405.
(52) Carboni, M.; Abney, C. W.; Liu, S.; Lin, W. Highly Porous and Stable Metal−Organic Frameworks for Uranium Extraction. *Chem. Sci.* **2013**, *4*, 2396−2402.
(53) Das, S.; Pandey, A. K.; Athawale, A. A.; Subramanian, M.; Seshagiri, T. K.; Khanna, P. K.; Manchanda, V. K. Silver Nanoparticles Embedded Polymer Sorbent for Preconcentration of Uranium from Bio-Aggressive Aqueous Media. *J. Hazard. Mater.* **2011**, *186*, 2051−2059.

DOI: 10.1021/am507361x
ACS Appl. Mater. Interfaces 2015, 7, 4589−4594